

Scenario and Model Dependence of Strategic Solar Climate Intervention in CESM

J. T. Fasullo and J. H. Richter

National Center for Atmospheric Research, Boulder, CO, USA.

Contents of this file

Figures S1 to S7

Introduction

These supporting figures provide further insight into the radiative responses in unmitigated warming scenarios in CESM1-WACCM5-RCP85 and CESM2-WACCM6-SSP585, the CESM1-LE and CESM2-LE, CESM2-RCP85, and the target geoengineered climate state in GLENS-SAI and ARISE-SAI-1.5. They also document rapid adjustments to CO₂ of clouds and radiation in CESM1 and CESM2 based on idealized 4xCO₂AMIP and abrupt4xCO₂ coupled simulations differences with AMIP and pre-industrial control simulations (see Table 1 of the main text). These figures thus provide key context for the interpretation of SAI uncertainties provided in the main text discussion.

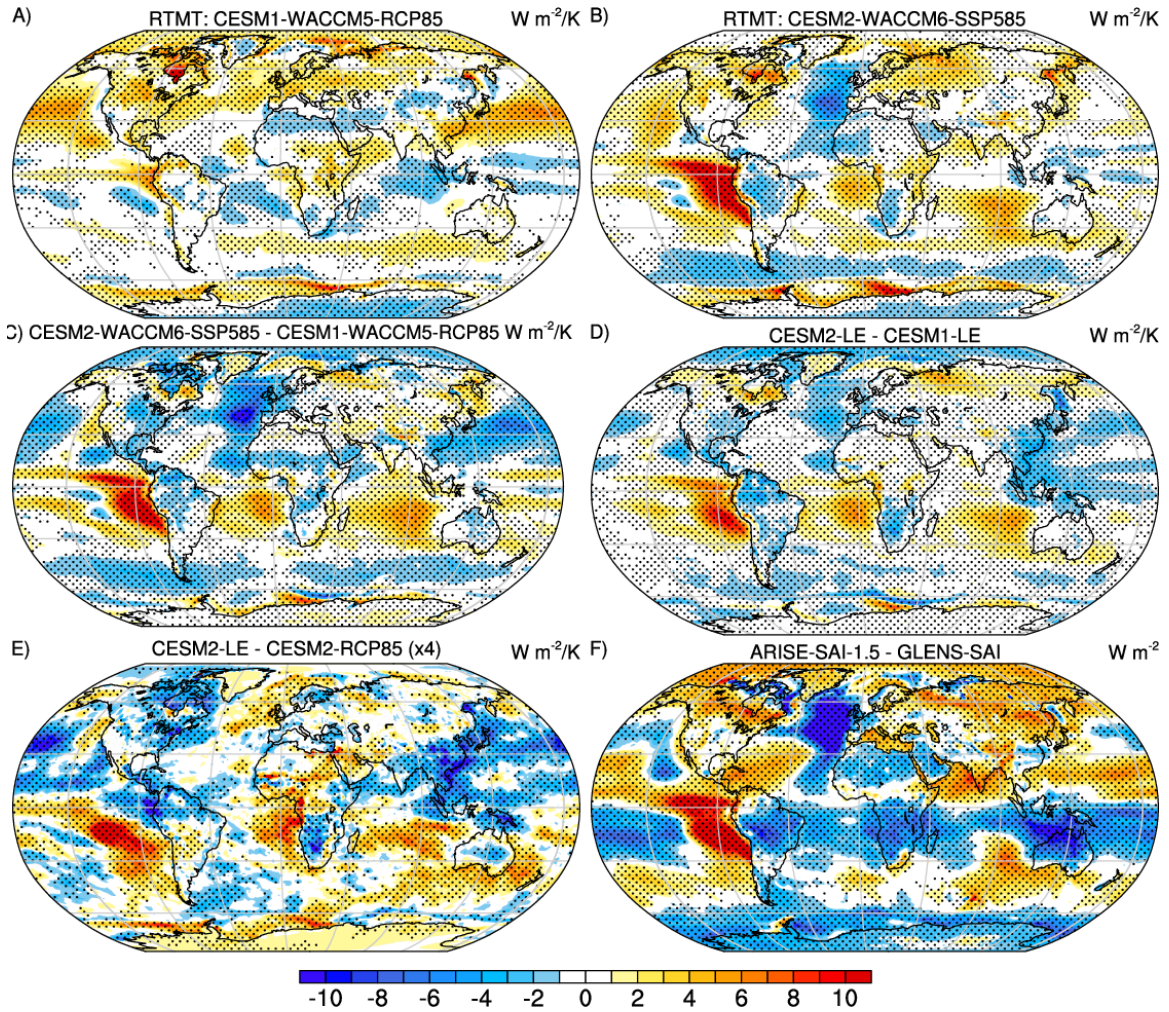


Figure S1. Normalized response in net top-of-atmosphere radiative flux (RTMT) estimated from the change between 2020-39 and 2050-69 per degree global warming for unmitigated (a) CESM1-WACCM5-RCP85 and (b) CESM2-WACCM6-SSP585 simulations, and (c) their difference (b-a). Also shown is (d) the analogous difference for the CESM1-LE and CESM2-LE and (e) the CESM2-RCP85 and CESM2-LE (scaled by 4). The difference between the geoengineered climate states in ARISE-SAI-1.5 and GLENS-SAI is shown in (f). Units for all panels are $\text{W m}^{-2} \text{K}^{-1}$, except in (f) where units are W m^{-2} , and stippled regions indicate differences that exceed twice the ensemble standard error.

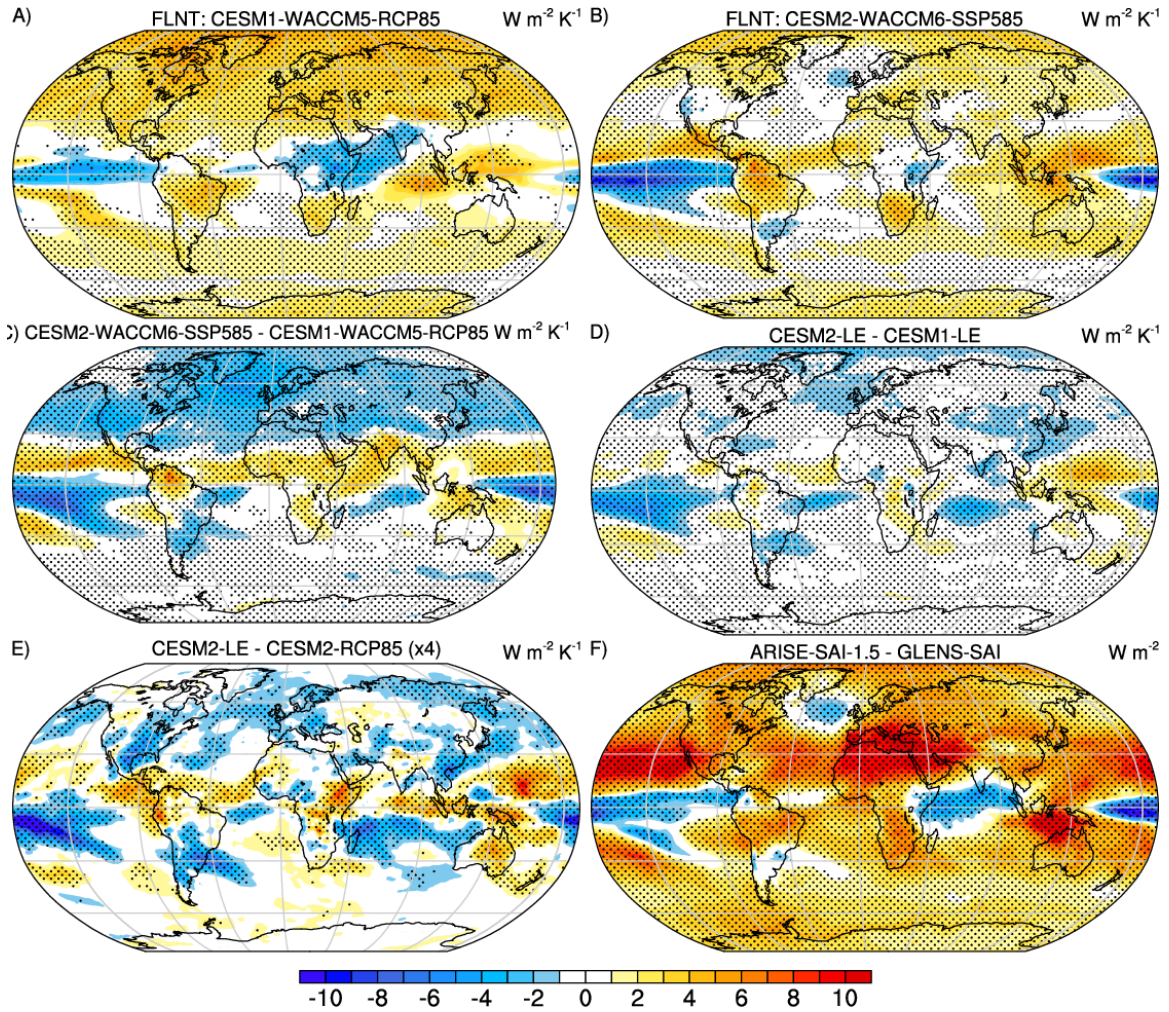


Figure S2. Normalized response in outgoing top-of-atmosphere longwave flux (FLNT) per degree global warming estimated from the change between 2020-39 and 2050-69 for unmitigated (a) CESM1-WACCM5-RCP85 and (b) CESM2-WACCM6-SSP585 simulations, and (c) their difference (b-a). Also shown is (d) the analogous difference for the CESM1-LE and CESM2-LE and (e) the CESM2-RCP85 and CESM2-LE (scaled by 4). The difference between the geoengineered climate states in ARISE-SAI-1.5 and GLENS-SAI is shown in (f). Units for all panels are $\text{W m}^{-2} \text{K}^{-1}$, except in (f) where units are W m^{-2} , and stippled regions indicate differences that exceed twice the ensemble standard error.

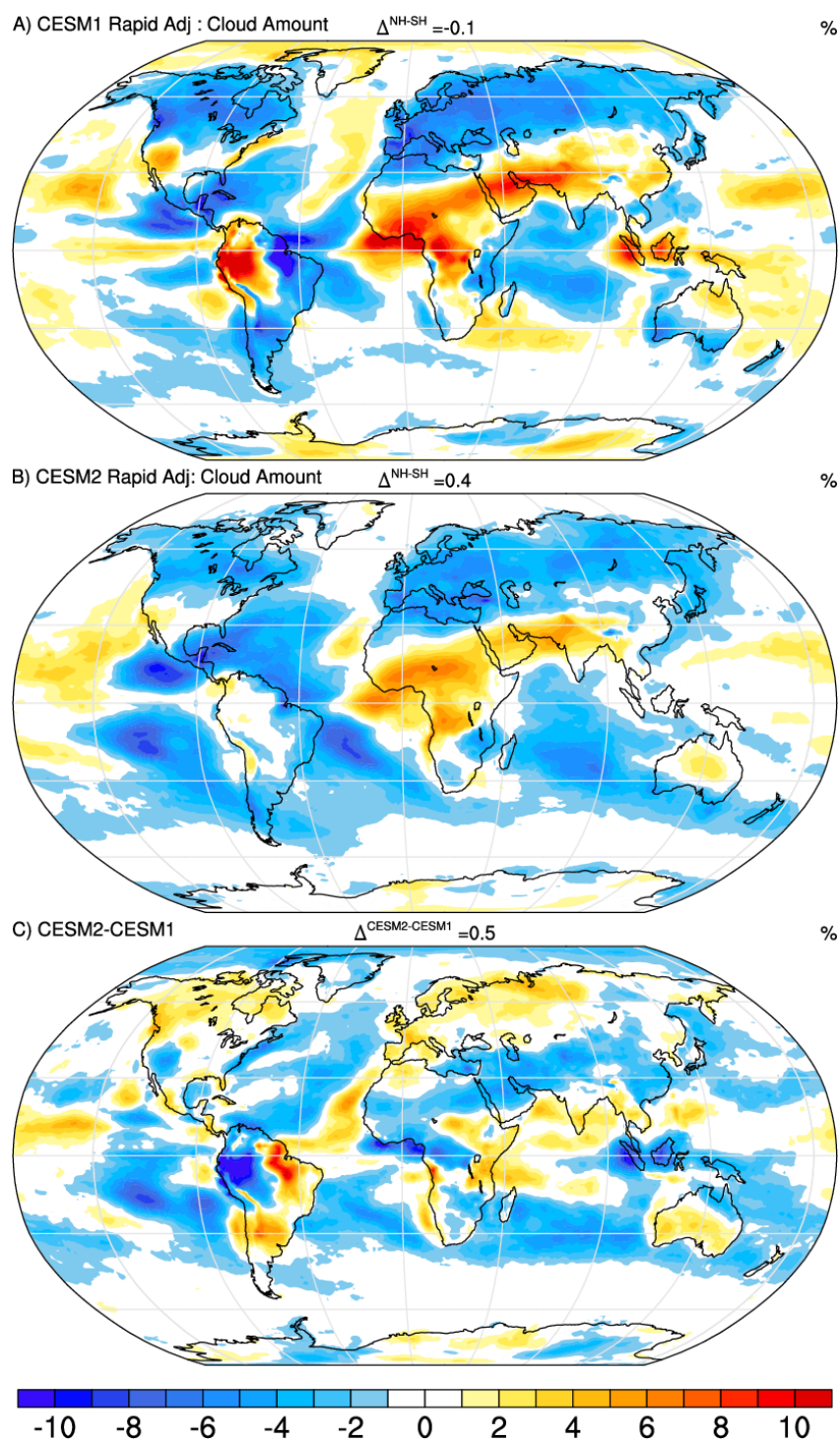
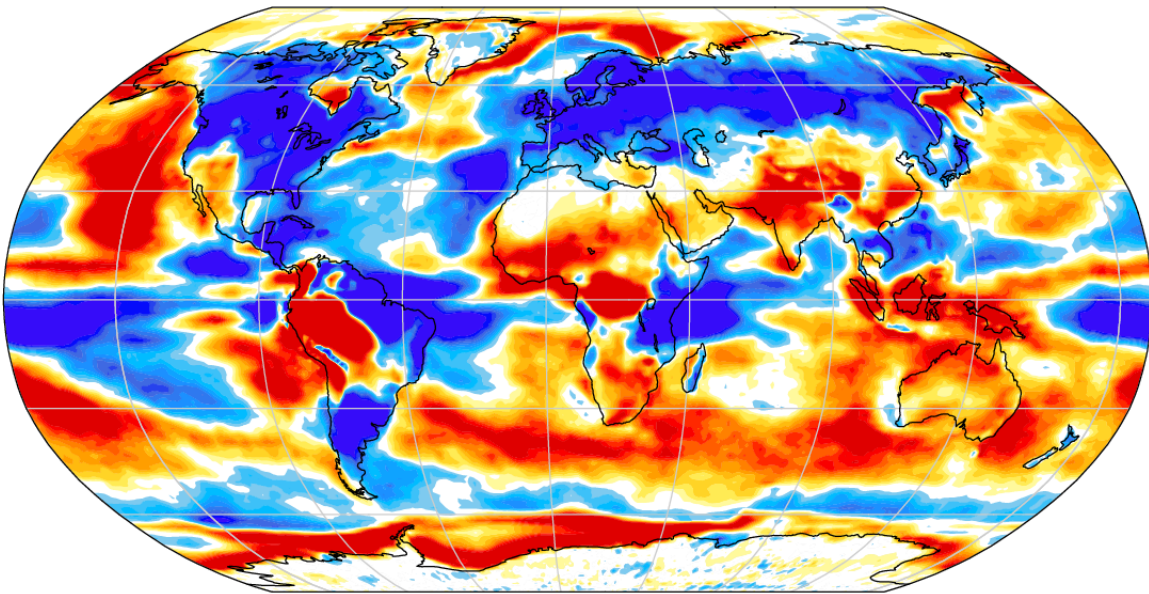


Figure S3. Rapid adjustments of cloud amount (%) to CO₂ based on 4xCO₂AMIP-AMIP simulation differences in (a) CESM1, (b) CESM2, and (c) their difference (b-a).

A) CESM1 Slow Response (Est): FSNT $\Delta^{NH-SH} = -2.3$ $W m^{-2}$



B) CESM2 Slow Response: FSNT $\Delta^{NH-SH} = -0.1$

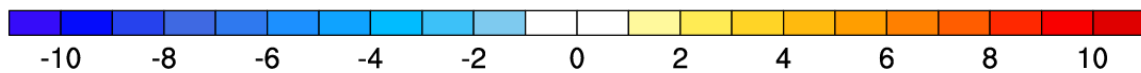
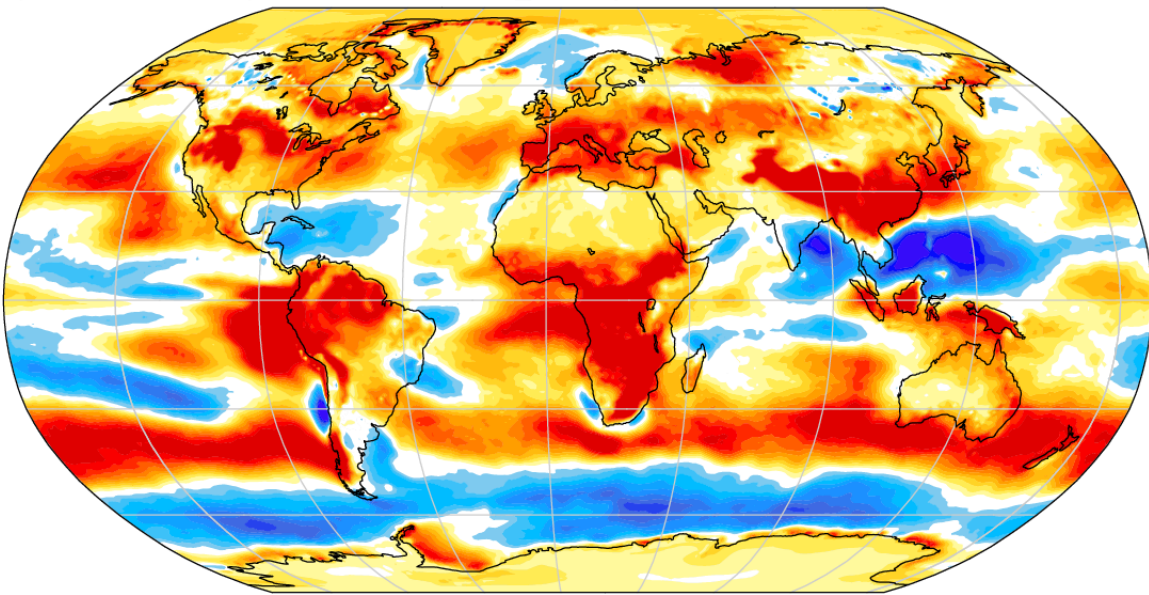


Figure S4. Slow responses of FSNT ($W m^{-2}$) to CO_2 estimated from abrupt4x CO_2 simulations in CESM1 (a), and computed directly from AMIP+4K-AMIP simulation differences in CESM2 (b). The hemispheric contrasts are large for CESM1 ($-2.3 W m^{-2}$) and small for CESM2 ($0.1 W m^{-2}$).

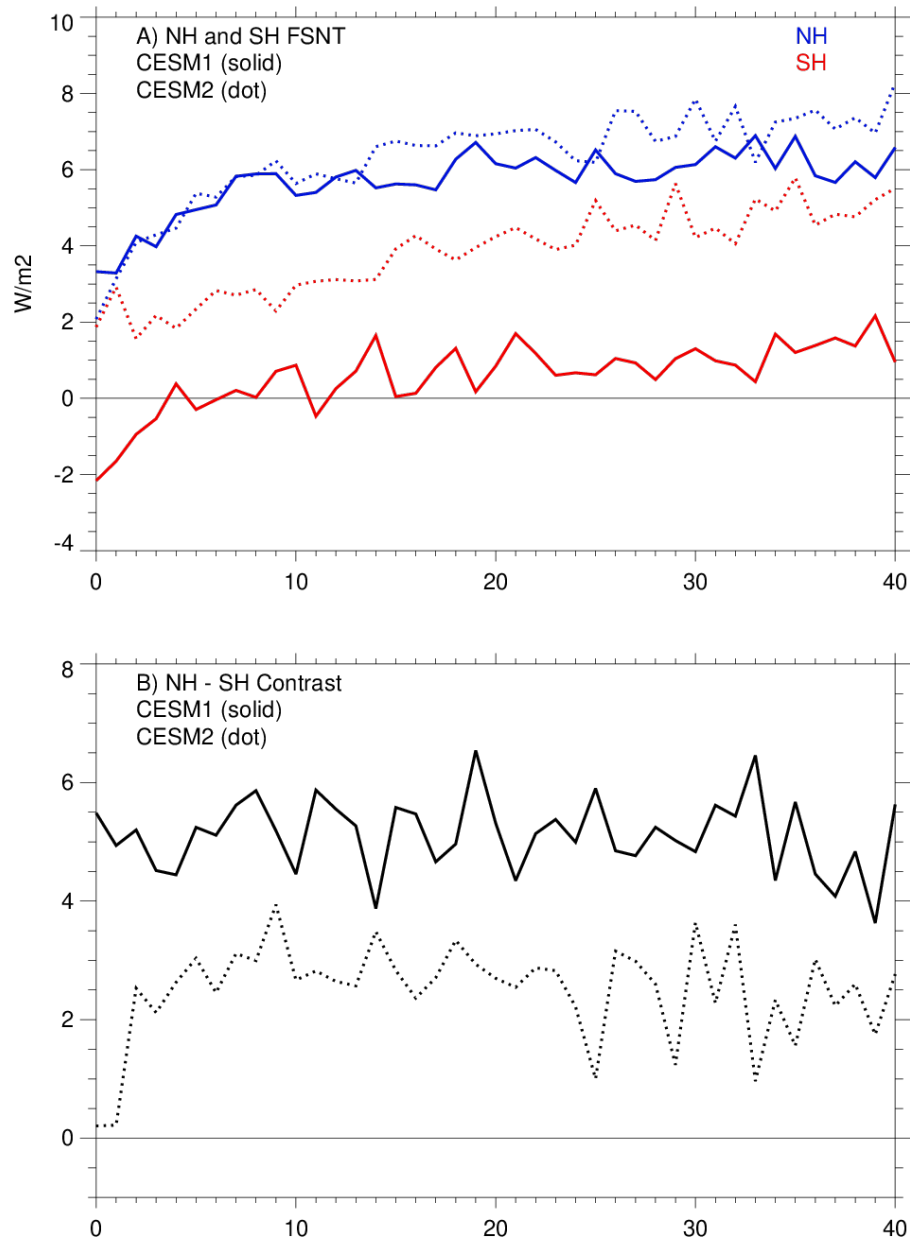


Figure S5. Timeseries of hemispheric mean fluxes (a) and their differences (b) in abrupt4xCO2 simulations.

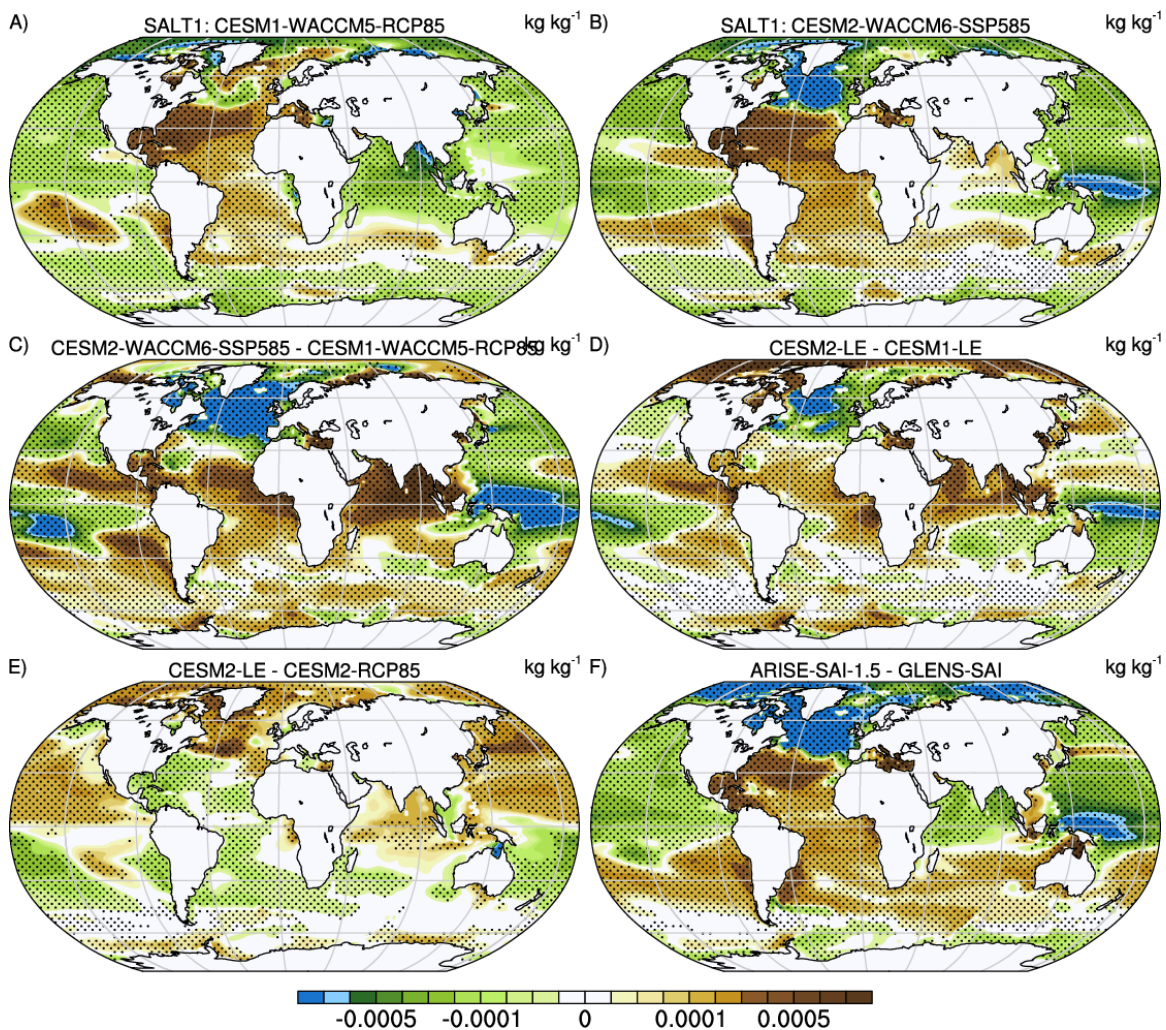


Figure S6. Response in surface salinity estimated from the change between 2020-39 and 2050-69 for unmitigated (a) CESM1-WACCM5-RCP85 and (b) CESM2-WACCM6-SSP585 simulations, and their difference (c). Also shown is the analogous difference for (d) the CESM1-LE and CESM2-LE (d) and (e) the CESM2-RCP85 and CESM2-LE. The difference between the geoengineered climate states in ARISE-SAI-1.5 and GLENS-SAI is shown in (f).

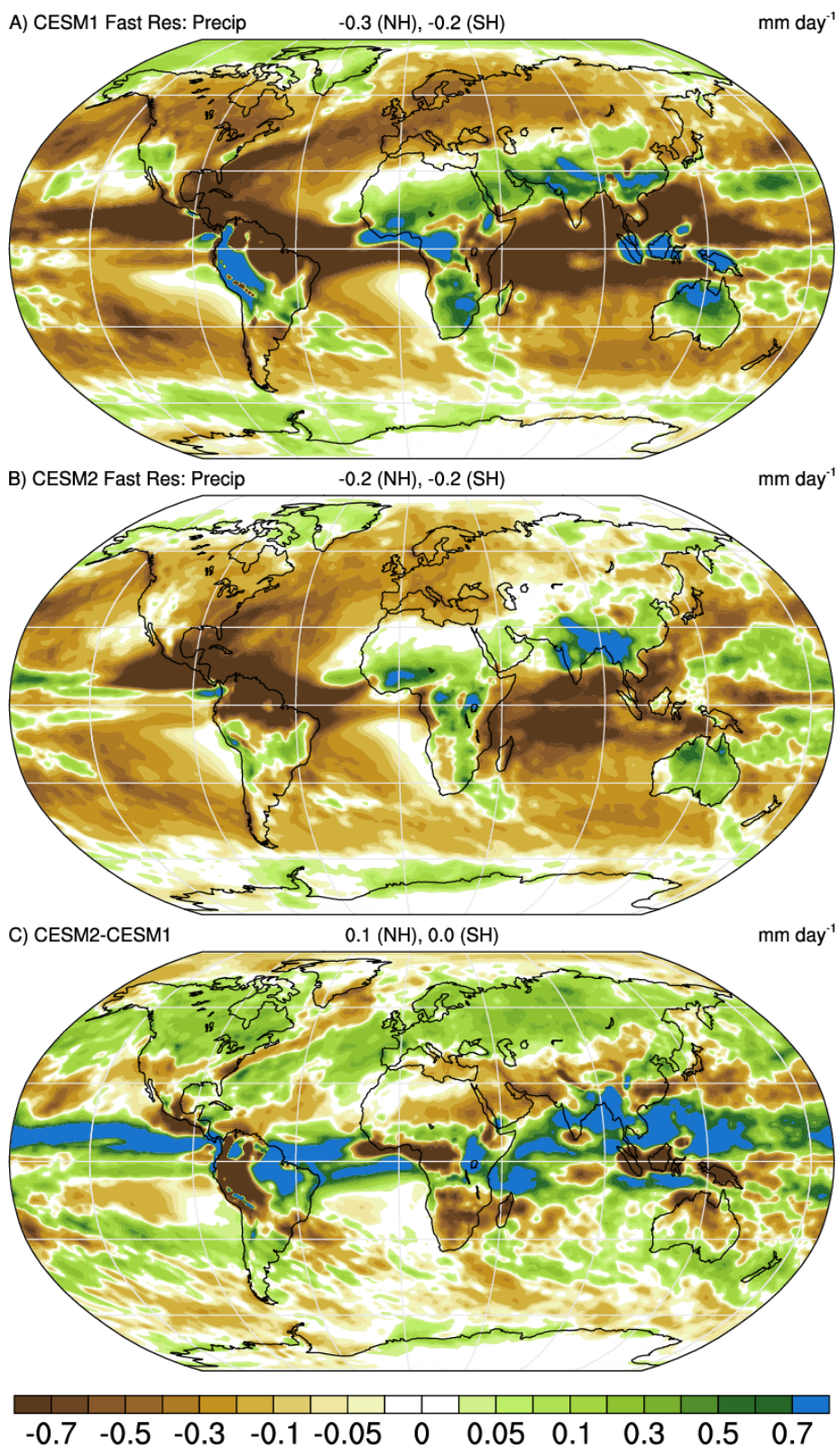


Figure S7. Rapid adjustments of precipitation (mm day⁻¹) to CO₂ based on 4xAMIP-AMIP simulation differences in (a) CESM1, (b) CESM2, and (c) their difference (b-a).